Design of Near-Infrared Dyes Based on π-Conjugation System Extension. Theoretical Evaluation of Arylimidazole Derivatives of Perylene Chromophore

Masafumi Adachi* and Yukinori Nagao†

Mitsubishi Chemical Corporation, Yokohama Research Center, 1000 Kamoshida-cho, Aoba-ku, Yokohama 227-8502, Japan

Received January 26, 1999. Revised Manuscript Received May 20, 1999

To design the near-infrared (NIR) dyes, the electronic absorption spectra of arylimidazole-introduced 3,4,9,10-perylenetetracarboxylic dianhydride and its imide derivatives (PTCAIs) have been theoretically elucidated by using the molecular orbital (MO) calculation. An arylimidazole introduction causes a longer shift of the absorption wavelength (bathochromic shift) by destabilization of the HOMO level. The HOMO level of aryl groups (e.g., benzene and naphthalene) is close to the energy of PTCAI's HOMO; therefore, new orbitals which are characterized as a mixture of each orbital's features are generated by this large orbital interaction. The absorption wavelength shift depends not only on a HOMO level of the aryl group (π-conjugation size), but also on its pattern. With the bathochromic shift of the absorption spectrum, the transition is characterized as more intense of the charge-transfer (CT) property rather than the π−π* excitation on the perylene moiety.

1. Introduction

Near-infrared (NIR) materials research is one of the important fields in material science. Moreover, NIR materials (e.g., dyes and pigments) have been noted as the key component in many applications and devices, spanning from electronic to biological fields.[1] In particular, laser diodes emit the NIR beam; therefore, NIR absorbing materials have been used in many of opt-electronic devices, for example laser printers and digital copy machines use the NIR-absorbing pigment as the charge-generation material (CGM) in their photoreceptors[1b,c] and optical disks (e.g., CD-R) are coated with a NIR absorbing dye for the memory layer.[1b,d] In the biological applications, NIR fluorescence dyes have been applied as indicators in the assay systems;[1a] moreover, NIR dyes have been used for photodynamic therapy (PDT) in the treatment of cancer.[1a,b] For commercial applications of materials, stability (light, heat, oxidation, etc.) is generally required, but in the mild condition, the most NIR materials are instable, except for the phthalocyanines and their analogues. Phthalocyanines have been widely used in many applications,[2] but the adaptation to photoemitting devices is difficult because of their low photoluminescence efficiency. Nowadays, the highly photoluminescent, and also environmentally stable, NIR materials are strongly required. 3,4,9,10-Perylenetetracarboxylic dianhydride and its imide derivatives (PTCAIs, simply called a perylene or a perylene chromophore in some cases) have been already recognized as the stable highly fluorescent chromphores.[3] Therefore, PTCAI derivatives can be looked upon as one of the candidates of new NIR materials for such applications.

PTCAIs are one of the important classes of dyes and pigments, used in many practical applications,[4] e.g., industrial pigments,[4b] laser dyes,[4f] photoreceptors of copiers,[4c] solar cells,[4d] and others. The PTCAI's solution absorbs the visible light with three sharp peaks (526, 489, and 458 nm in $CHCl_3$);[3j] neither the absorption wavelength nor the intensity is affected by the change of its imide substituents.[3] In contrast, the color as the pigment (solid state) largely depends on the imide structure, because the imide controls the intermolecular

* E-mail: ada@rc.m-kagaku.co.jp. FAX: +81-45-963-3978.

† Faculty of Science and Technology, Science University of Tokyo, 2641 Yamazaki, Noda 278-8510, Japan.

(1) (a) Daehne, S., Resch-Genger, U., Wolfbeis, O. S., Eds. *Near-Infrared Dyes for High Technology Applications*; Kluwer Academic Publishers: Dordrecht, 1998. (b) Fabian, J.; Nakazumi, H.; Matsuoka, M. *Chem. Rev.* **1992**, *92*, 1197. (c) Law, K.-Y. *Chem. Rev.* **1993**, *93*, 449. (d) Peng, Z.; Geise, H. J. *Bull. Soc. Chim. Belg.* **1996**, *105*, 739. (e) Burkinshaw, S. M.; Hallas, G.; Towns, A. D. *Rev. Prog. Color. Relat. Top.* **1996**, *26*, 47.

(2) Leznoff, C. C., Lever, A. B. P., Eds. *Phthalocyanines Properties and Applications*; VCH: New York, 1989, 1993, 1993, 1996; Vols. 1−4.

(3) (a) Rademacher, A.; Märkle, S.; Langhals, H. *Chem. Ber.* **1982**, *115*, 2927. (b) Langhals, H. *Chem. Ber.* **1985**, *118*, 4641. (c) Demmig, S.; Langhals, H. *Chem. Ber.* **1988**, *121*, 225. (d) Ebeid, El-Z. M.; El-Daly, S. A.; Langhals, H. *J. Phys. Chem.* **1988**, *92*, 4565. (e) Langhals, H.; Fünfschilling, J.; Glatz, D.; Zschokke-Gränacher, I. *Spectrochim. Acta* **1988**, *44A*, 311. (f) Langhals, H.; Demmig, S.; Huber, H. *Spectrochim. Acta* **1988**, *44A*, 1189. (g) Kaiser, H.; Lindner, J.; Langhals, H. *Chem. Ber.* **1991**, *124*, 529. (h) Johansson, L. B.-Å.; Langhals, H. *Spectrochim. Acta* **1991**, *47A*, 857. (i) Deligeorgiev, T.; Zaneva, D.; Petkov, I.; Timcheva, Il.; Sabnis, R. *Dyes Pigm.* **1994**, *24*, 75. (j) Adachi, M.; Murata, Y.; Nakamura, S. *J. Phys. Chem.* **1995**, *99*, 14240. (k) Mercadante, R.; Trsic, M.; Duff, J.; Aroca, R. *J. Mol. Struct. (THEOCHEM)* **1997**, *394*, 215.

(4) (a) Krasovitskii, B. M.; Bolotin, B. M. *Organic Luminescent Materials*; VCH: Weinheim, 1988. (b) Herbst, W.; Hunger, K. *Industrial Organic Pigments*, 2nd ed.; VCH: Weinheim, 1997. (c) Popovic, Z. D.; Loutfy, R. O.; Hor, Ah-M. *Can. J. Chem.* **1985**, *63*, 134. (d) Panayotatos, P.; Parikh, D.; Sauers, R.; Bird, G.; Piechowski, A.; Husain, S. *Solar Cells* **1986**, *18*, 71. (e) Seybold, G.; Wagenblast, G. *Dyes Pigm.* **1989**, *11*, 303. (f) Sadrai, M.; Hadel, L.; Sauers, R. R.; Husain, S.; Krogh-Jespersen, K.; Westbrook, J. D.; Bird, G. R. *J. Phys. Chem.* **1992**, *96*, 7988.

10.1021/cm990051z CCC: $18.00
Published on Web 07/28/1999

interaction at the solid state and determines the crystal packing.[4b,5] PTCAI dyes (molecule); moreover, pigments (solid state), do not show the sensitivity in the NIR region.[3−5]

A long time is needed to synthesize and evaluate new materials, but they do not always satisfy the predicted properties. Theoretical studies (calculations), however, can be done in a shorter period of time, without expensive regents, and without dangers. Presently, we are required speed up research and development (R&D) and commercializing of new materials. If we combine, integrate, and utilize theoretical calculations with R&D of material science, we shall see gains because theoretical studies can provide basic concepts and guiding principles of the material design, also contribute to speedier screening before synthesis.

In this study, we theoretically elucidate the absorption spectra of perylene derivatives and evaluate them as new NIR material candidates. It has been generally accepted that an increase in the size of the π-conjugation causes a shift toward a longer absorption wavelength (bathochromic shift).[6] To design the NIR dyes, there are two ways of the PTCAI π-conjugation system extension: an arylimidazole introduction[7−9] and a perylene framework extension.[10] In this paper, we theoretically analyze the absorption spectrum shift by using the semiempirical MO INDO/S method,[11] focusing on the arylimidazole introduction.

Many types of arylimidazole-introduced PTCAIs have been synthesized and reported their properties and applications,[7] but solubility of these molecules is generally low. As a result, their absorption spectra have not been clearly elucidated and details of the absorption spectrum shift have not been characterized. Recently, soluble monoarylimidazole-introduced PTCAIs were synthesized by comprehensive protocols, and their absorption spectra were reported by our group[8] and Langhals et al.[9] We compare the observed and calculated spectra and discuss the possibility of new NIR material design.

2. Calculation Method

We analyzed absorption spectra of PTCAI **1** and many kinds of arylimidazole-introduced dyes **2**−**8** (Chart 1) by MO calculations.[12] In the first step, the molecular structures of dyes **1**−**8** were optimized by the AM1 method using the MOPAC program package.[13] We did not use any construction in the optimized process, but all optimized structures were nearly planar except the sterically hindered points.[14]

The equilibrium structures were then employed in the second step to calculate the absorption spectra by the INDO/S method.[11] In this method, which is a modified INDO version for absorption spectrum calculations, integrals were evaluated with the Nishimoto−Mataga formula[15] and SCF calculations were executed at the closed-shell Hatree−Fock level (RHF). Configuration interaction (CI) calculations were performed to include single excited configurations from the ground state, consisting of 35 (occupied orbitals) × 35 (virtual orbitals) configurations.

3. Results and Discussion

A. Benzimidazole Introduction. At the first, we consider the benzimidazole introduction as a typical aryl group. It has been already experimentally and theoretically shown that the imide substituents of PTCAI do not affect the absorption spectrum as the molecule;[3] therefore, we have selected the H atom to replace the imide substituent in the calculations. Table 1 summarizes the observed and calculated absorption spectra of PTCAI **1**, mono and bis benzimidazole introduced dyes **2**−**4**.[16] By introducing the benzimidazole moiety, the absorption maximum (λ_{max}) is shifted to a longer wavelength (bathochromic shift, Table 1).

Figure 1 shows the transition energy (reciprocal value of the λ_{max}), HOMO → LUMO excitation energy ($E_{HOMO\rightarrow LUMO}$), and HOMO−LUMO energy gap ($\Delta\epsilon_{HOMO,LUMO}$) of dyes **1**−**4**. The transition property of all dyes can be described by the HOMO → LUMO excitation (Table 1), and the transition energy shift synchronizes with the HOMO → LUMO excitation energy change (Figure 1). As a result, the bathochromic shift can be explained by their HOMO and LUMO properties.

(5) (a) Klebe, G.; Graser, F.; Hädicke, E.; Berndt, J. *Acta Crystallogr.* **1989**, *B45*, 69. (b) McKerrow, A. J.; Buncel, E.; Kazmaier, P. M. *Can. J. Chem.* **1993**, *71*, 390. (c) Kazmaier, P. M.; Hoffmann, R. *J. Am. Chem. Soc.* **1994**, *116*, 9684. (d) Erk, P.; Hetzenegger, J.; Böhm, A. *Eur. Coat. J.* **1997**, 906.

(6) (a) Orchin, M.; Jaffé, H. H. *Symmetry, Orbitals, and Spectra*; Wiley-Interscience: New York, 1971. (b) Griffiths, J. *Colour and Constitution of Organic Molecules*; Academic Press: London, 1976. (c) Fabian, J.; Hartmann, H. *Light Absorption of Organic Colorants*; Springer-Verlag: Berlin, 1980. (d) Zollinger, H. *Color Chemistry*, 2nd ed.; VCH: Weinheim, 1991.

(7) (a) Lukác, I.; Langhals, H. *Chem. Ber.* **1983**, *116*, 3524. (b) Popovic, Z. D.; Hor, Ah-M.; Loutfy, R. O. *Chem. Phys.* **1988**, *127*, 451. (c) Loutfy, R. O.; Hor, A. M.; Kazmaier, P.; Tam, M. *J. Imag. Sci.* **1989**, *33*, 151. (d) Fujita, Y.; Adachi, C.; Tsutsui, T.; Saito, S. *Nippon Kagaku Kaishi* **1992**, 1154. (e) Quante, H.; Geerts, Y.; Müllen, K. *Chem. Mater.* **1997**, *9*, 495.

(8) (a) Nagao, Y.; Ishikawa, N.; Tanabe, Y.; Misono, T. *Chem. Lett.* **1979**, 151. (b) Nagao, Y.; Ishikawa, N.; Tanabe, Y.; Misono, T. *Nippon Kagaku Kaishi* **1980**, 1391. (c) Nagao, Y.; Misono, T. *Dyes Pigm.* **1984**, *5*, 171.

(9) Langhals, H.; Sprenger, S.; Brandherm, M.-T. *Liebigs Ann.* **1995**, 481.

(10) (a) Désilets, D.; Kazmaier, P. M.; Burt, R. A. *Can. J. Chem.* **1995**, *73*, 319. (b) Désilets, D.; Kazmaier, P. M.; Burt, R. A.; Hamer, G. K. *Can. J. Chem.* **1995**, *73*, 325. (c) Quante, H.; Müllen, K. *Angew. Chem., Int. Ed. Engl.* **1995**, *34*, 1323. (d) Langhals, H.; Schönmann, G.; Feiler, L. *Tetrahedron Lett.* **1995**, *36*, 6423. (e) Holtrup, F. O.; Müller, G. R. J.; Quante, H.; De Feyter, S.; De Schryver, F. C.; Müllen, K. *Chem. Eur. J.* **1997**, *3*, 219. (f) Rohr, U.; Schlichting, P.; Böhm, A.; Gross, M.; Meerholz, K.; Bräuchle, C.; Müllen, K. *Angew. Chem., Int. Ed. Engl.* **1998**, *37*, 1434. (g) Geerts, Y.; Quante, H.; Platz, H.; Mahrt, R.; Hopmeier, M.; Böhm, A.; Müllen, K. *J. Mater. Chem.* **1998**, *8*, 2357.

(11) (a) Ridley, J.; Zerner, M. *Theor. Chim. Acta* **1973**, *32*, 111. (b) Ridley, J. E.; Zerner, M. C. *Theor. Chim. Acta* **1976**, *42*, 223. (c) Bacon, A. D.; Zerner, M. C. *Theor. Chim. Acta* **1979**, *53*, 21. (d) Zerner, M. C.; Loew, G. H.; Kirchner, R. F.; Mueller-Westerhoff, U. T. *J. Am. Chem. Soc.* **1980**, *102*, 589.

(12) We consider the molecular structure of dye **6** (mono-1,2-naphthimidazole introduction) is as shown in the figure, because another geometrical isomer is unstable by the steric interaction.

(13) (a) Dewar, M. J. S.; Zoebisch, E. G.; Healy, E. F.; Stewart, J. J. P. *J. Am. Chem. Soc.* **1985**, *107*, 3902. (b) MOPAC Ver. 5, Stewart, J. J. P. *QCPE Bull.* **1989**, *9*, 10.

(14) The optimized molecular structures of mono-1,8-naphthimidazole **7** and 9,10-phenanthimidazole **8** dyes twist between the perylene part and the aryl group (**7**, 23°; **8**, 10°) by the steric interaction.

(15) (a) Nishimoto, K.; Mataga, N. *Z. Phys. Chem. (Neue Folge)* **1957**, *12*, 335. (b) Mataga, N.; Nishimoto, K. *Z. Phys. Chem. (Neue Folge)* **1957**, *13*, 140.

(16) In some cases, INDO/S calculations underestimate the absorption wavelength, especially for organic dyes and pigments. We have previously proposed the relationship between the observed and calculated λ_{max}: $\lambda_{max}(obs) = 1.65\lambda_{max}(calc) - 187$ (nm). Adachi, M.; Nakamura, S. *Dyes Pig.* **1991**, *17*, 287. The scaled absorption wavelength almost reproduces the observed λ_{max}, for examples, the scaled value of the calculated λ_{max} for PTCAI **1** is 541 nm and for mono benzimidazole dye **2** is 589 nm.

Table 1. Observed and Calculated Absorption Spectra of PTCAI and Its Benzimidazole Derivatives

	observed		calculated (INDO/S)		
dye[a]	λ_{max} (nm)	ϵ_{max}	λ_{max} (nm)	f[b]	transition property[c]
1 (PTCAI)	526[d]	81 500	441	1.258	−0.981{(HOMO, 70) → (LUMO, 71)}
2 (mono)	571[e]	57 400	470	1.467	−0.957{(HOMO, 83) → (LUMO, 84)}
3 (*trans*-bis)	605[f]	22 900	486	1.801	0.958{(HOMO, 96) → (LUMO, 97)}
4 (*cis*-bis)	605[f]	22 900	491	1.719	0.958{(HOMO, 96) → (LUMO, 97)}

[a] R = H, for dyes **1** and **2** in calculation. [b] Oscillator strength. [c] Excitations having the CI coefficient over 0.25 are shown. [d] R = 2-ethylhexyl, in $CHCl_3$ solution, ref 3j. [e] R = 1-hexylheptyl, in $CHCl_3$ solution, ref 9. [f] *tert*-Butyl-substituted benzimidazole, cis−trans mixture, in DMF solution, ref 7a.

Chart 1

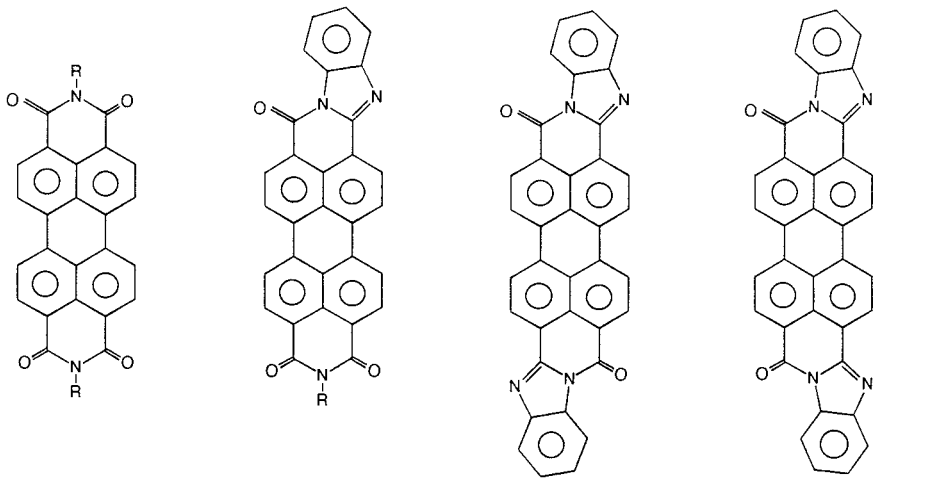

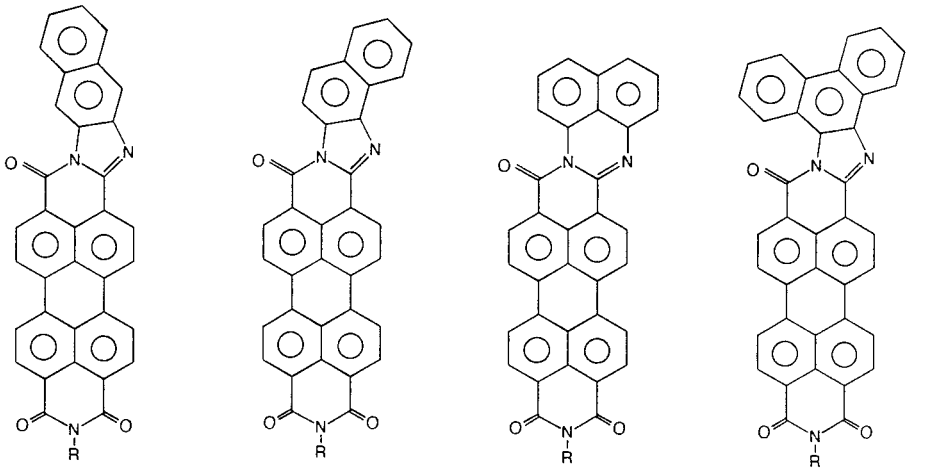

Singlet HOMO → LUMO excitation energy ($^1E_{HOMO\rightarrow LUMO}$) is expressed by using the electronic interaction terms J and K:

$$^1E_{HOMO\rightarrow LUMO} = \Delta\epsilon_{HOMO,LUMO} - J_{HOMO,LUMO} + 2K_{HOMO,LUMO}$$

where $\Delta\epsilon$ is the HOMO−LUMO energy gap; J, the Coulomb integral; and K, the exchange integral.

Each component of the $^1E_{HOMO\rightarrow LUMO}$ for dyes **1**−**4** is summarized in Table 2. By introducing the benzimidazole, the HOMO−LUMO energy gap ($\Delta\epsilon_{HOMO,LUMO}$) is narrowed to almost the same amount as the HOMO → LUMO excitation energy reduction. In contrast, the electronic interaction term ($J - 2K$) is nearly constant (Table 2 and Figure 1). Figure 2 illustrates HOMOs and LUMOs of dyes **1**−**4** with their energy levels. The HOMO energy level largely rises with the benzimidazole introduction, because the HOMO delocalizes whole in the molecule; however, both the LUMO level and its pattern are almost same. As a result, this bathochromic shift should be explained by the HOMO property.

B. Mechanism of Orbital Energy Shift. Figure 3 illustrates the orbital correlation diagram between PTCAI **1**, its monobenzimidazole-introduced dye **2**, and benzene. Figures 4 and 5 show important frontier orbitals of PTCAI **1** and dye **2**, respectively. Figure 3 clearly indicates that the benzene HOMOs (doubly

Table 2. Detail of HOMO → LUMO Excitation Properties of PTCAI and Its Benzimidazole Derivatives (INDO/S)

dye[a]	transition energy[b] (cm^{-1})	$^1E_{HOMO\rightarrow LUMO}$[c] ($cm^{-1}$)	$\Delta\epsilon_{HOMO,LUMO}$[d] ($cm^{-1}$)	$J_{HOMO,LUMO}$[e] (cm^{-1})	$2K_{HOMO,LUMO}$[f] (cm^{-1})	$J-2K$ (cm^{-1})	ϵ_{HOMO}[g] (au)	ϵ_{LUMO}[g] (au)
1 (PTCAI)	22 660	23 970	44 530	28 860	8 300	20 560	−0.290 88	−0.088 00
2 (mono)	21 260	23 010	42 270	25 220	5 960	19 260	−0.276 74	−0.084 14
3 (*trans*-bis)	20 560	22 290	41 300	24 890	5 880	19 010	−0.268 76	−0.080 58
4 (*cis*-bis)	20 370	22 110	41 130	24 650	5 630	19 020	−0.267 96	−0.080 58

[a] R = H, for dyes **1** and **2**. [b] Energy expression of the λ_{max}. [c] Singlet excitation energy. [d] Deference of orbital energies. [e] Coulomb integral. [f] Exchange integral. [g] Orbital energy.

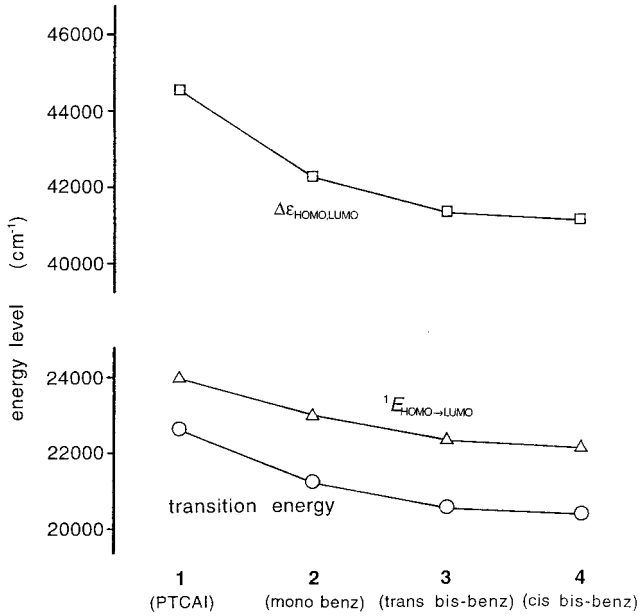

Figure 1. Transition energy, singlet HOMO → LUMO excitation energy ($^1E_{HOMO\rightarrow LUMO}$), and HOMO−LUMO energy gap ($\Delta\epsilon_{HOMO,LUMO}$) of PTCAI **1** and its benzimidazole derivatives **2**−**4** (INDO/S).

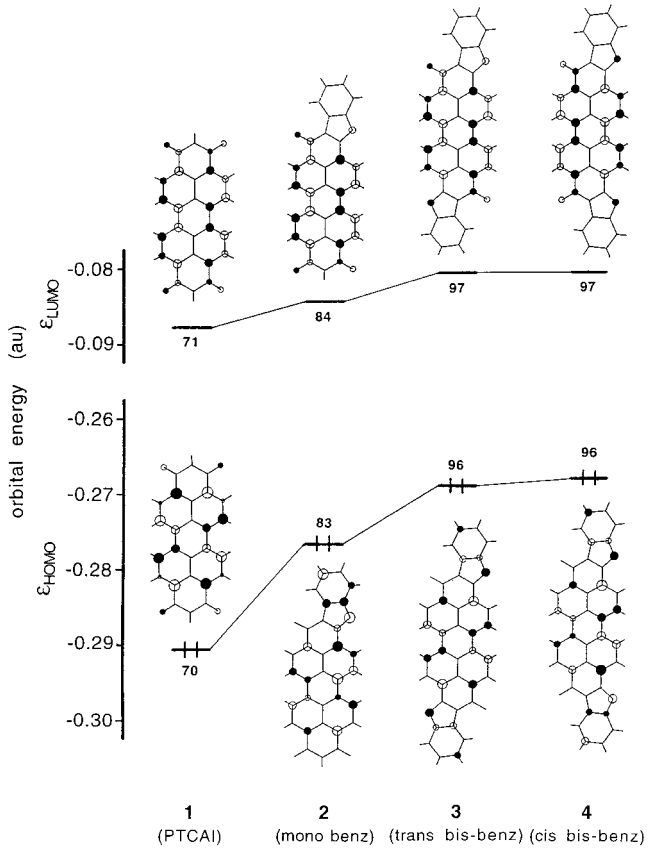

Figure 2. HOMOs and LUMOs of PTCAI **1** and its benzimidazole derivatives **2**−**4** (INDO/S).

degeneration) are near in the PTCAI HOMO level, thus these orbitals interact. As a result, three new orbitals arise on monobenzimidazole dye **2** (orbitals 81−83, Figures 2−5). The HOMO of dye **2** can be characterized as the slightly perturbed PTCAI's HOMO by one of the benzene HOMOs (Figure 2). Since the connecting point (=N−C− bond) between the perylene and the benzene is antibonding in character (Figure 2), the HOMO of dye **2** becomes slightly unstable. The HOMO-1 (82nd) and HOMO-2 (81st) orbitals of dye **2** are mainly characterized as the benzene HOMOs with small contribution of the PTCAI's HOMO property (Figures 3 and 5). Neither the energy levels nor the patterns of the orbitals 77−80 of dye **2** are affected by the benzimidazole introduction (Figures 3−5), because the next HOMO of benzene (−0.45651 au) completely separates from these orbitals.

In the contrast with HOMO, the LUMO of dye **2** is not affected by the benzimidazole introduction. The energy level of benzene LUMOs (doubly degeneration, +0.03093 au) largely separates from low-lying virtual orbitals of PTCAI **1** (71−75th, Figure 3); therefore, the interaction can be negligible. As a result, both the energy levels and their patterns of low-lying virtual orbitals (84−88th) of dye **2** are almost the same, corresponding PTCAIs' (71−75th, Figures 2−5). We conclude that the HOMOs' interaction between PTCAI and benzene causes the bathochromic shift.

Bisbenzimidazole-introduced dyes (**3** and **4**) can be simply regarded as further benzimidazole-introduced systems to dye **2**; therefore, their absorption spectrum shifts can be explained in the same manner.

C. Comparison of Absorption Spectra: PTCAI and Monobenzimidazole Dye. The calculated absorption spectra, including subtransitions and n−π* transitions, of PTCAI **1** and its monobenzimidazole-introduced dye **2** are summarized in Tables 3 and 4. The state dipole moments of transitions, which are indexes of the charge transfer (CT) strength, are almost zero upon PTCAI **1** by its symmetrical molecular structure (Table 3). In contrast with PTCAI, the ground and excited states' dipole moments of dye **2** are varying nonzero values (2−14 D, Table 4), which mean nonequivalent charge-transfer strengths in each state. For example, the lowest energy transition (470 nm) is characterized by moderate CT strength (7.9 D). On the other hand, the next lowest energy transition (381 nm), which corresponds neither of the transitions of PTCAI **1** (Table 3), connotes large CT character (13.7 D), since the predominant property is an excitation from the benzimidazole part (82nd orbital) to the perylene moiety (LUMO) (Table 4 and Figures 2 and 5).

Despite a larger π-conjugation size of dye **2**, λ_{max} of the subtransition (345 nm, *f*: 0.012) is nearly same as

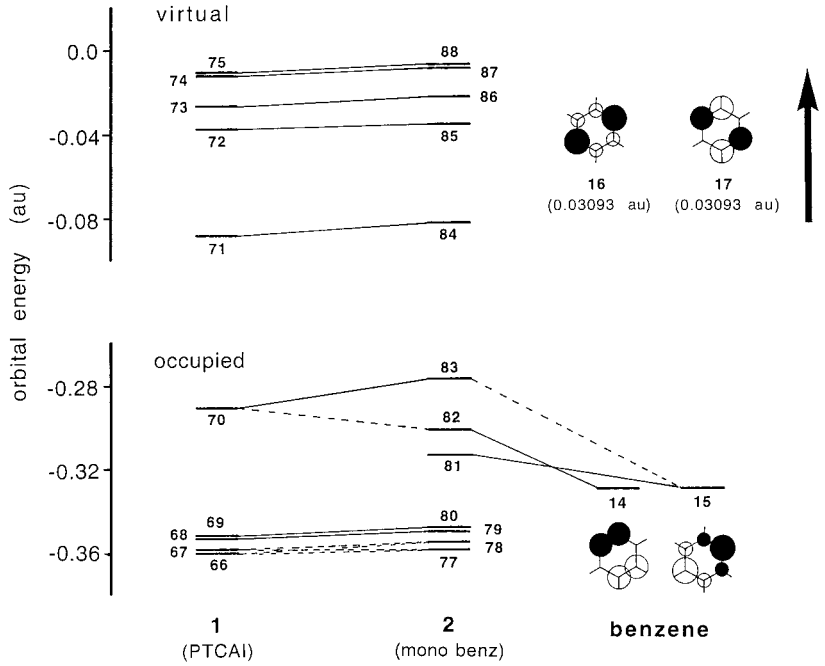

Figure 3. Frontier molecular orbital energy diagram of PTCAI **1**, its monobenzimidazole derivative **2**, and benzene (INDO/S).

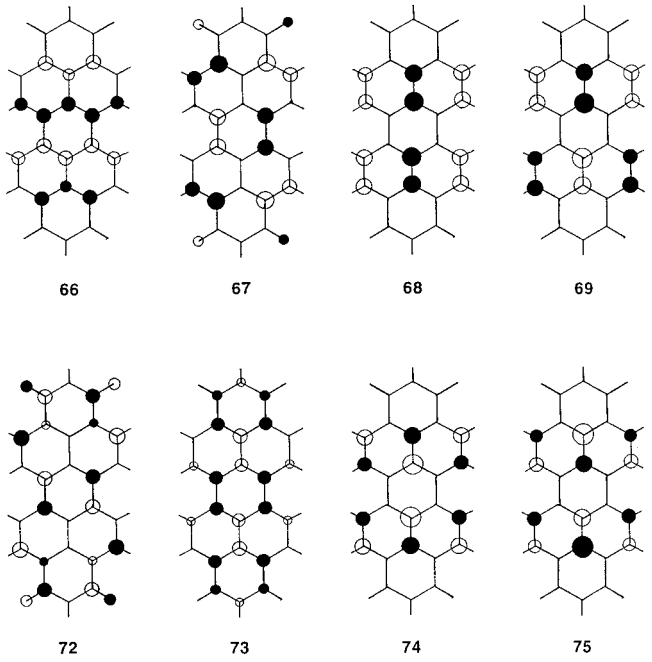

Figure 4. Frontier molecular orbitals of PTCAI **1** (INDO/S).

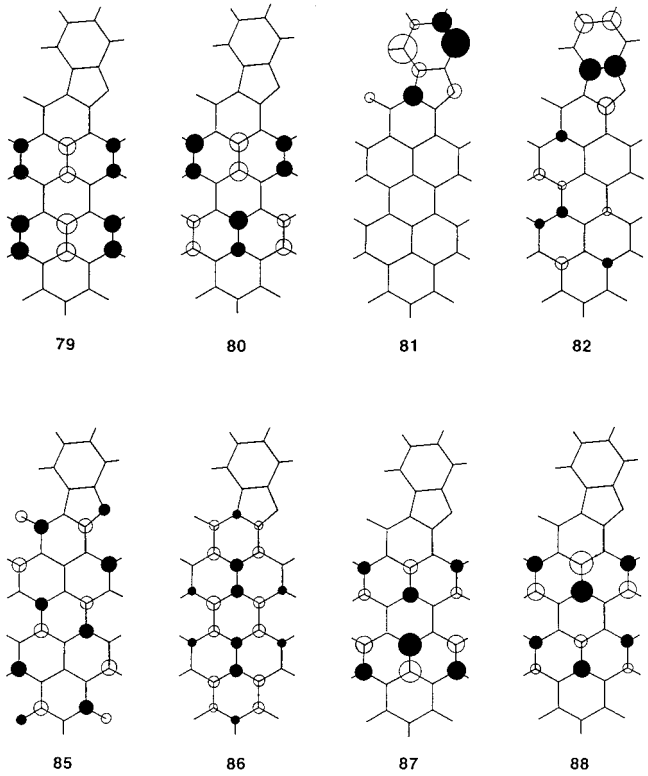

Figure 5. Frontier molecular orbitals of monobenzimidazole derivative **2** of PTCAI (INDO/S).

that of PTCAI **1** (344 nm, *f*: 0.022). We have already elucidated that the PTCAI **1** subtransition originates from the naphthalene B_{3u} transition (along naphthalene long axis).[3j] The π-conjugation size of dye **2** is same as that of dye **1** for the subtransition; therefore, almost the same subtransition band appears. Moreover, we can understand its small state dipole moment (2.6 D, Table 4) by its transition property (intra-perylene transition). The calculated 350-nm band of dye **2** with a small state dipole moment (3.3 D, Table 4) corresponds to the 347 nm transition of PTCAI **1** (Table 3), because both are characterized as the forbidden type sub transitions.[3j]

Four n$-\pi^*$ transitions of PTCAI **1** are located on 355$-$373 nm (Table 3), on the other hand, only three transitions appear in its monobenzimidazole dye **2** in corresponding region (Table 4). These n$-\pi^*$ bands are characterized by the transitions that consist of the carbonyl O atoms' lone pair orbitals moving toward π^* orbitals excitations.[3j] One carbonyl moiety is displaced by the benzimidazole in dye **2**, therefore, the transition concerning this part is replaced by the new n (N atom lone pair orbital)$-\pi^*$ transition, whose energy level is high.

D. Various Arylimidazoles Introduction. Table 5 shows the absorption spectra of various arylimidazoles mono-introduced perylenes. It has been generally ac-

Table 3. Detail of Absorption Spectrum of PTCAI 1 (R = H, INDO/S)

λ_{max} (nm)	f[a]	dipole moment[b] (D)	transition property[c]
		0.00[d]	
441	1.258	0.00	−0.981 {(HOMO, 70) → (LUMO, 71)}
373	0.001	0.66	(n-π*)
373	0.000	0.66	(n-π*)
355	0.000	0.50	(n-π*)
355	0.000	0.50	(n-π*)
347	0.000	0.00	0.739 {69 → 71}
			−0.548 {70 → 74}
344	0.022	0.00	0.701 {68 → 71}
			0.583 {70 → 75}

[a] Oscillator strength. [b] State dipole moment. [c] Excitations having the CI coefficient over 0.25 are shown. [d] Ground state.

Table 4. Detail of Absorption Spectrum of Monobenzimidazole Derivative 2 (R = H, INDO/S)

λ_{max} (nm)	f[a]	dipole moment[b] (D)	transition property[c]
		2.45[d]	
470	1.467	7.93	−0.957 {(HOMO, 83) → (LUMO, 84)}
381	0.047	13.65	−0.850 {82 → 84}
371	0.001	2.55	(n-π*)
367	0.001	7.55	(n-π*)
353	0.000	1.94	(n-π*)
350	0.000	3.26	−0.646 {80 → 84}
			−0.445 {83 → 87}
			−0.366 {83 → 88}
345	0.012	2.58	−0.610 {79 → 84}
			−0.439 {83 → 88}
			0.284 {83 → 87}
332	0.009	11.88	−0.541 {81 → 84}
			0.456 {83 → 85}
			−0.418 {83 → 86}
325	0.018	10.88	−0.499 {81 → 84}
			0.484 {83 → 86}
			0.275 {81 → 85}
			−0.262 {83 → 85}

[a] Oscillator strength. [b] State dipole moment. [c] Excitations having the CI coefficient over 0.25 are shown. [d] Ground state.

cepted that a larger π-conjugated molecule absorbs the longer wavelength light (bathochromic shift).[6] But, the λ_{max} of 2,3-naphthimidazole dye **5** is not bathochromic shift from benzimidazole dye **2** (slightly hypsochromic shift at the observation[9] and almost same λ_{max} at the calculation, Table 5). On the other hand, the absorption bands of 1,2-naphthimidazole dye **6** and 1,8-naphthimidazole dye **7** show larger bathochromic shifts than benzimidazole dye **2** and 2,3-naphthimidazole dye **5** (Table 5).

To elucidate the remarkable absorption spectral difference between the isomers of naphthimidazole dyes **5**−**7**, we compare detail of these transition properties (Table 6). As the first step, we focus on HOMO → LUMO excitation properties, because the transitions can be roughly characterized by the HOMO → LUMO excitations (Table 5). Since the electronic term ($J - 2K$) is almost the same value for dyes **5**−**8**, the excitation energy difference can be explained by the HOMO−LUMO energy gap (Table 6). Narrower HOMO−LUMO gaps of dyes **6** and **7** are a reason for the larger bathochromic shifts. We investigate the mechanism of the orbital energy shift by analyzing orbital correlation diagrams of PTCAI **1** and naphthalene. The interaction between HOMOs of PTCAI **1** and naphthalene should be generally large, because both HOMOs are almost degenerate (Figures 6 and 7). What other property determines the orbital interaction? Positions 1, 4, 5, and 8 of naphthalene have large pronounce lobes on its HOMO; therefore, the interaction between PTCAI **1** and 1,8-naphthimidazole must be large (Figure 6), thus two generated orbitals widely split.[17] The largely unstabilized HOMO of 1,8-naphthimidazole dye **7** almost localizes upon the naphthalene moiety; therefore, the longest absorption band is pronounced bathochromic shift with much CT character (19.0 D, Table 5). While positions 2, 3, 6, and 7 slightly contribute to the naphthalene HOMO, hence the small split two orbitals arise by the 2,3-naphthimidazole introduction (dye **5**, Figure 7). The absorption band of dye **5** is slightly bathochromic shift than PTCAI **1** with little CT character (8.9 D, Table 5), because the HOMO does not localize upon the naphthalene moiety (Figure 7). These results clearly indicate that the HOMO level shifted by the arylimidazoles introduction is controlled by not only relative orbital energy levels, but also by an orbital pattern of the aryl group. In contrast with HOMO, the LUMO levels of dyes **5** and **7** are almost same as that of PTCAI **1**, because the LUMO of naphthalene is laying at a remarkably higher energy level than that of PTCAI **1** (Figures 6 and 7).

Electronic terms ($J - 2K$) of the HOMO → LUMO excitation of naphthimidazole introduced dyes **5**-**7** (16 300−17 200 cm^{-1}, Table 6) are smaller than of benzimidazole dye **2** (19 300 cm^{-1}, Table 2), because the distances between arylimidazole part (pronounced on HOMO) and perylene moiety (LUMO) in naphthimidazole dyes **5**−**7** are longer by their extended π-conjugations. Generally, a decrease of the electronic term ($J - 2K$) should cause a hypsochromic shift, but the mixing of the other excitations (CI effect) in dyes **5**−**7** almost cancels this effect (see transition and HOMO → LUMO excitation energies of dyes **2** and **5** in Tables 2, 5, and 6).

The observed λ_{max} of 9,10-phenanthimidazole-introduced dye **8** is 583 nm[9] (midway between the values of 2,3-naphthimidazole **5** and 1,8-naphthimidazole **7** dyes), but the calculated value largely shifts to longer (523 nm, Table 5) than naphthimidazole dyes **5**−**7**. The solubility of 9,10-phenanthimidazole dye **8** should be low by its large π-conjugation. Although the λ_{max} of dye **8** was reported in ref 9, but neither the absorption spectrum nor the molar extinction coefficient was shown. Therefore, we consider one of the reasons of the discrepancy between the observed and calculated λ_{max} may be low resolution of the observed absorption spectrum of dye **8**.

E. Arylimidazole Introduced Dyes as Materials. The absorption and luminescence spectra of PTCAI **1** (without arylimidazoles) are remarkably sharp, which are characterized by three distinct vibronic bands.[3] The chromophoric system of PTCAI **1** is a symmetrical rigid structure, therefore, only a few vibronic bands have the pronounced intensity. On the other hand, the arylimidazoles introduction causes the absorption spectral

(17) The molecular structure of 1,8-naphthimidazole dye **7** slightly twists at the imidazole moiety (23°). This distortion causes stabilization of the HOMO energy level, because both connecting points between the perylene chromophore and the naphthalene are antibonding properties (Figure 6). Therefore, this nonplanarity does not concern the longer absorption wavelength, but instead contributes to a hypsochromic shift.

Table 5. Observed and Calculated Absorption Spectra of PTCAI and Its Monoarylimidazole Derivatives

	observed		calculated (INDO/S)				
dye[a]	λ_{max} (nm)	ϵ_{max}	λ_{max} (nm)	f[b]	dipole moment (D)[c]	transition property[d]	
1 (PTCAI)	526[e]	81 500	441	1.258	0.00	−0.981 {(HOMO, 70) → (LUMO, 71)}	(23 970)
2 (benz)	571[f]	57 400	470	1.467	7.93	−0.957 {(HOMO, 83) → (LUMO, 84)}	(23 010)
5 (2,3-naphth)	567[f]	48 800	471	1.682	8.94	0.830 {(HOMO, 92) → (LUMO, 93)}	(24 330)
						0.453 {91 → 93}	(27 330)
6 (1,2-naphth)			505	1.211	15.86	0.904 {(HOMO, 92) → (LUMO, 93)}	(22 370)
7 (1,8-naphth)	604[f]		505	1.062	18.99	−0.872 {(HOMO, 92) → (LUMO, 93)}	(22 530)
						−0.319 {92 → 94}	(31 900)
						−0.276 {91 → 93}	(25 190)
8 (9,10-phenanth)	583[f]		523	0.934	18.90	0.905 {(HOMO, 101) → (LUMO, 102)}	(21 720)
						0.286 {101 → 103}	(31 730)

[a] R = H, in calculation. [b] Oscillator strength. [c] Excited-state dipole moment. [d] Excitations having the CI coefficient over 0.25 are shown. Value in parentheses shows generated configuration ($i \rightarrow j$) excitation energy ($^1E_{i\rightarrow j}$, cm^{-1}). [e] R = 2-ethylhexyl, in $CHCl_3$ solution, ref 3j. [f] R = 1-hexylheptyl, in $CHCl_3$ solution, ref 9.

Table 6. Detail of HOMO → LUMO Excitation Properties of Monoarylimidazole Derivatives (INDO/S)

dye[a]	transition energy[b] (cm^{-1})	$^1E_{HOMO\rightarrow LUMO}$[c] ($cm^{-1}$)	$\Delta\epsilon_{HOMO,LUMO}$[d] ($cm^{-1}$)	$J_{HOMO,LUMO}$[e] (cm^{-1})	$2K_{HOMO,LUMO}$[f] (cm^{-1})	$J - 2K$ (cm^{-1})	ϵ_{HOMO}[g] (au)	ϵ_{LUMO}[g] (au)
5 (2,3-naphth)	21 240	24 330	41 040	20 070	3 360	16 710	−0.271 30	−0.084 32
6 (1,2-naphth)	19 800	22 370	39 530	20 010	2 850	17 160	−0.264 17	−0.084 06
7 (1,8-naphth)	19 810	22 530	38 850	18 270	1 950	16 320	−0.259 04	−0.082 01
8 (9,10-phenanth)	19 100	21 720	38 720	19 320	2 320	17 000	−0.259 62	−0.083 19

[a] R = H. [b–g] See footnotes of Table 2.

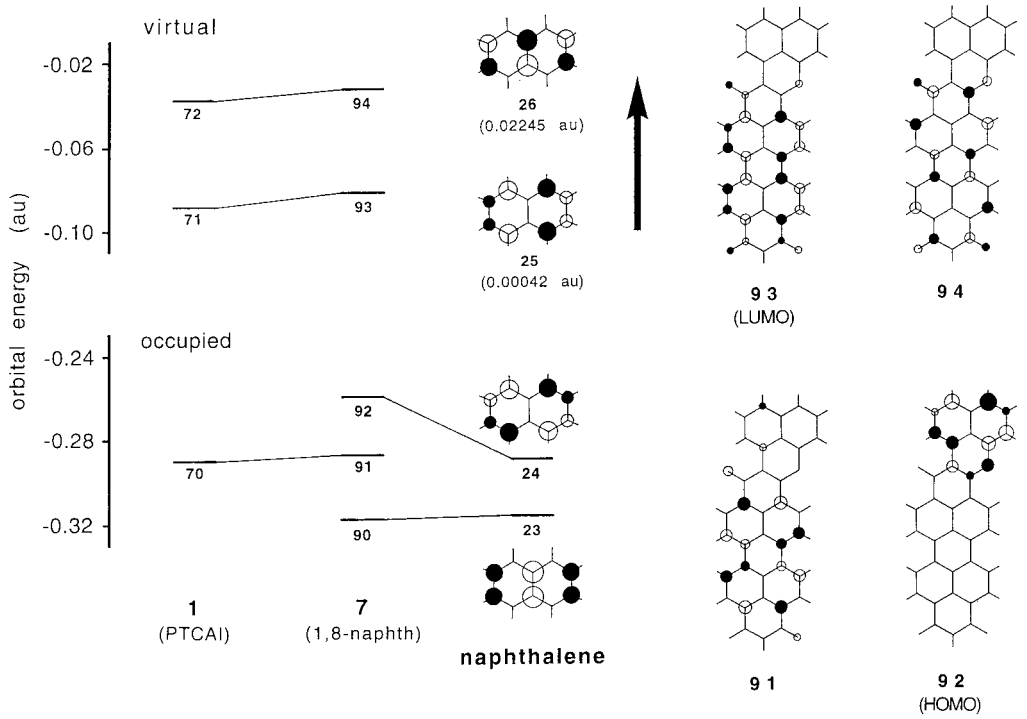

Figure 6. Frontier molecular orbital energy diagram of PTCAI **1**, its mono-1,8-naphthimidazole derivative **7**, and naphthalene (INDO/S).

broadening.[7–9] A dull spectrum shape is generally undesirable, because some practical applications, e.g., dye lasers, optical filters, optical-disks, and so on, strictly require the spectral sharpness of materials. The molecule symmetry is lowered by the arylimidazoles introduction, as a result, many vibronic bands should have intensity and the spectrum shape becomes broad.[18] Bromine substitution at the arylimidazole moiety again causes the spectral narrowing, we consider one of the reasons may be the change of vibronic transition properties by introducing the heavy atom such as Br.

Finally, we discuss the arylimidazole-introduced perylenes as NIR materials. The orbital interaction between HOMOs of the perylene and the aryl group at the substituted point causes the bathochromic shift, in other words, their absorption properties can be looked upon as the perturbed perylene system. Moreover, many kinds of arylimidazole-introduced dyes have been evaluated their absorption properties (see section 3.D, Table 5, and refs 7−9), but none of the dyes absorb NIR light.[19] These results strongly suggest that the bathochromic

(18) Poor resolution of the spectrum may be another reason for the dullness, because the solubility is lowering by the arylimidazoles introduction.

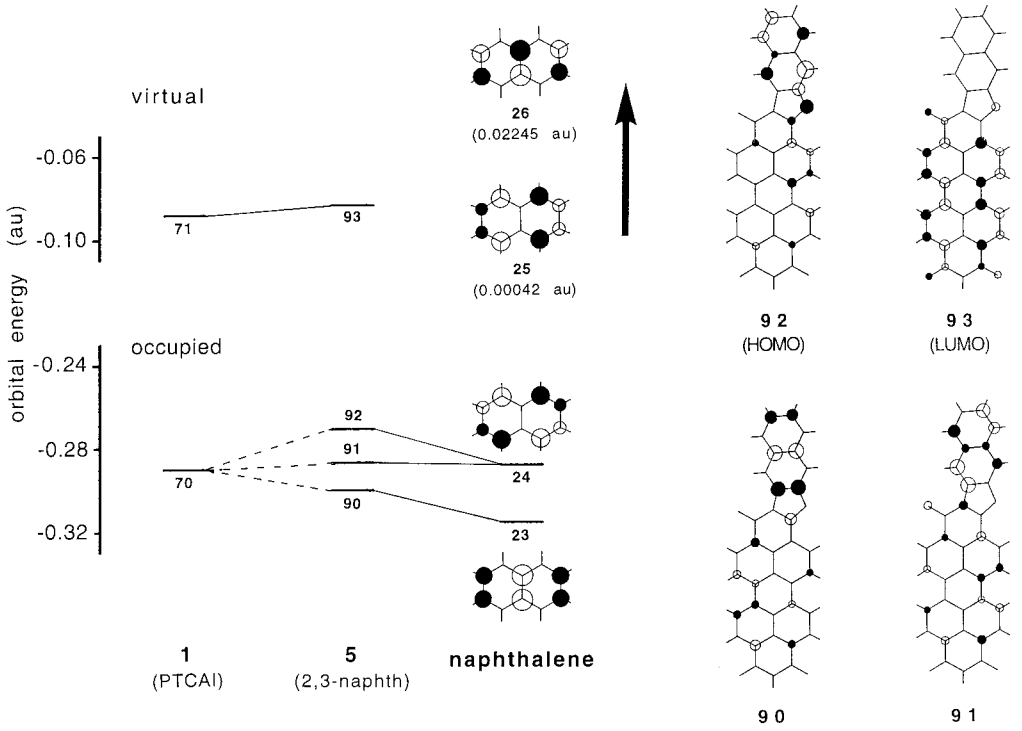

Figure 7. Frontier molecular orbital energy diagram of PTCAI **1**, its mono-2,3-naphthimidazole derivative **5**, and naphthalene (INDO/S).

shift is possible, but this shift is limited by their perylene framework.

Through this study, we conclude that the arylimidazole-introduced perylenes cannot be looked upon as new NIR-absorbing dye candidates. However, this result provides important information concerning the new NIR materials' design; we must not waste time in the aryl-group modification and should go the other way. The absorption spectra of polyaromatic molecules, like as a perylene chromophore, are mainly determined by their framework structures. Recently, quaterrylene- and terrylenetetracarboxylic dianhydride dyes have been synthesized, and these absorption spectra were reported.[10] From perylene, terrylene, to quaterrylene, the absorption spectra are largely bathochromic shifts to NIR region (terrylene 650 nm,[10e] quaterrylene 764 nm[10c]) retaining spectral sharpness, since longer π-conjugation sizes and symmetrical structures of their frameworks.

(19) In the solid state (pigment), occasionally bis-arylimidazole-introduced perylenes slightly absorb the NIR light, because the intermolecular interaction causes a bathochromic shift. But the solubility of such a system is extremely low; therefore, it cannot be used in applications as the dye.

4. Conclusion

We have analyzed the details of the longer absorption spectrum shift by the arylimidazoles introduction to the perylene chromophore. This bathochromic shift is roughly explained by the change of frontier orbital properties, especially the HOMO energy level. The HOMO level of an arylimidazole dye does not depend only on relative orbital levels of the perylene and the aryl group, but also on an orbital pattern of the aryl group. The aryl group influences the perylene chromophore as the perturbation.

Although the arylimidazoles introduction causes the bathochromic shift, but on the basis of its mechanism, room for the bathochromic shift should be limited. We conclude that the NIR-absorbing dye design based on the arylimidazoles introduction to the perylene chromophore is difficult, but it would be possible in the perylene π-framework extension (e.g., quaterrylene).[10]

Acknowledgment. The authors thank Professor M. C. Zerner for the release of the ZINDO program.

CM990051Z